Nanoparticle PEBBLE Sensors in Live Cells and In Vivo

Yong-Eun Koo Lee, Ron Smith, and Raoul Kopelman

Department of Chemistry, University of Michigan, Ann Arbor, Michigan 48109; email: yeleekoo@umich.edu, ronsgsmit@umich.edu, kopelman@umich.edu

Annu. Rev. Anal. Chem. 2009. 2:57–76

First published online as a Review in Advance on February 2, 2009

The *Annual Review of Analytical Chemistry* is online at anchem.annualreviews.org

This article's doi: 10.1146/annurev.anchem.1.031207.112823

1936-1327/09/0719-0057$20.00

Key Words

nanosensor, ion, molecule, ROS, fluorescence, SERS

Abstract

Nanoparticle sensors have been developed for real-time imaging and dynamic monitoring, both in live cells and in vivo, of molecular and ionic components, constructs, forces, and dynamics observed during biological, chemical, and physical processes. With their biocompatible small size and inert matrix, nanoparticle sensors have been successfully applied to noninvasive real-time measurements of analytes and fields in cells and in rodents, with spatial, temporal, physical, and chemical resolution. This review describes the diverse designs of nanoparticle sensors for ions and small molecules, physical fields, and biological features, as well as the characterization, properties, and applications of these nanosensors to in vitro and in vivo measurements. Their floating as well as localization abilities in biological media are captured by the acronym PEBBLE: photonic explorer for bioanalysis with biologically localized embedding.

1. INTRODUCTION

Fluorescence: emission of light caused by molecular absorption of incident light

Ratiometric measurement: technique wherein a signal is measured with respect to a reference signal

An ideal bioanalytical and biomedical sensor should achieve real-time tracking of biological, chemical, and physical processes both in live cells and in vivo. Such a sensor should also be able to detect disease-related abnormal features, with no interferences. Despite many efforts toward miniaturization, the large sizes of traditional (i.e., microelectrode and fiber optical) sensors make them far from ideal (1).

Fluorescent molecular probes have so far played a major role in intracellular sensing and imaging (2). Their fast response, their intense signal against relatively low background noise, and the relatively simple instrumental setup have made the molecular probe–based fluorescence technique a perfect match for real-time measurements in cells. However, these molecular probes have several drawbacks that affect the reliability of their intracellular measurements (3, 4). The probe molecules must be in a cell-permeable form, which often requires proper derivatization of the molecules that in itself might interfere with their function. The cytotoxicity or perturbed effects of the available dyes are often a problem, as the mere presence of these dye molecules may chemically interfere with the cell's processes. Intracellular measurements are often skewed by sequestration to specific organelles inside the cell or by nonspecific binding to proteins and other cell components. Furthermore, the dye is usually not ratiometric (i.e., it has only a single spectral peak), which requires technologically more demanding techniques, such as picosecond lifetime resolution and phase-sensitive detection, to be implemented. Note that merely loading a separate reference dye into the cell for ratiometric measurements is not a solution because of the aforementioned sequestration and nonspecific binding.

For in vivo applications, the impact of these drawbacks is even more severe. Only a subset of the molecular probes would reach a specific location of interest within the body, which is also a challenge for other systems such as drug delivery. This is also true for crossing biological barriers, such as the blood-brain barrier. Multiple drug resistance, caused by the ability of certain tumor cells to pump out small drug (or probe) molecules, is also a problem. Moreover, for in vivo optical methods, photons can only penetrate tissue to a limited depth. For deep-tissue imaging (millimeters to centimeters), one must use near-infrared (NIR) light in the spectral range of 650 to 900 nm, which is separated from the major absorption peaks of blood and water (5–7). The NIR region is free from autofluorescence of cellular components and is therefore advantageous for intracellular measurements as well. Note that most of the currently available molecular probes have visible absorption/emission wavelengths. Nanoparticle probes can be easily tailored for the NIR spectral range.

Advances in nanotechnology have made many types of nanoparticles available as platforms for constructing new types of bioanalytical sensors. The nanoparticles range from 1 to 1000 nm in size, thus causing minimal physical interference to cells. For example, a single spherical nanoparticle measuring 500 nm in diameter is at least four orders of magnitude smaller in volume than is a typical mammalian cell (8), and a 20-nm particle is eight orders of magnitude smaller. Most of the nanoparticle matrices are nontoxic, and therefore the nanoparticles do not cause chemical interference to cells. Delivery of nanoparticles into cells or animals can be performed via standard delivery methods. Intracellular delivery methods for nanoparticles, where the particles travel through the plasma membrane barrier, include picoinjection, gene gun delivery (9, 10), liposome incorporation (11), nonspecific or receptor-mediated endocytosis with surface-conjugated translocating proteins/peptides (12–14), and membrane-penetrating TAT peptides used by the human immumodeficiency virus (**Figure 1**) (15, 16). These delivery techniques cause negligible physical and chemical perturbation to the cell. For example, cell viability after gene gun delivery was found to be about 99% compared to that of control cells (11). Once delivered into cells, the sensors can

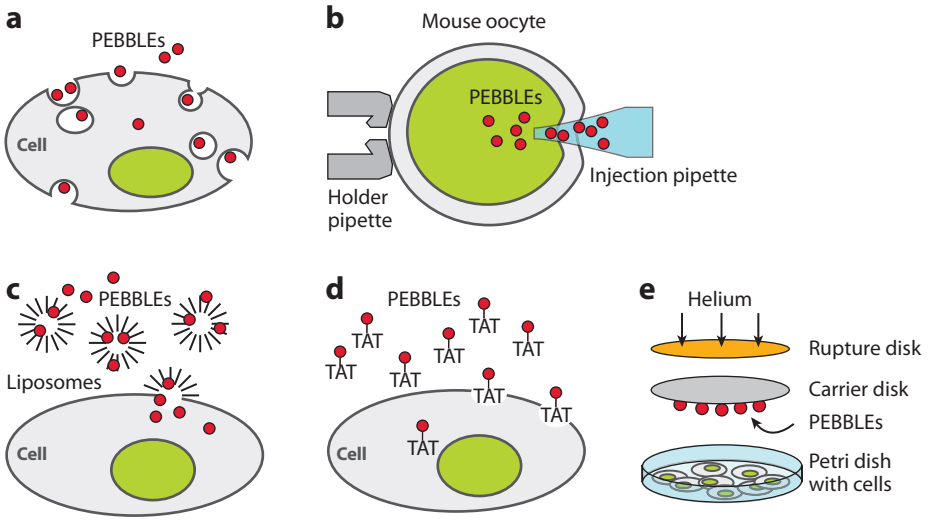

Figure 1

Methods of delivering nanoparticles into single cells for bioanalysis. (*a*) Endocytosis (nonspecific or receptor mediated). (*b*) Picoinjection. (*c*) Liposomal delivery. (*d*) Membrane-penetration peptide (TAT). (*e*) Gene gun. Abbreviation: PEBBLE, photonic explorer for bioanalysis with biologically localized embedding.

be used with conventional microscopy techniques, enabling high spatial and temporal resolution. For in vivo nanoparticle delivery, intravenous injection is typically used.

Due to their nontoxicity and excellent engineerability, nanoparticles have many advantages (4, 17) as building blocks for intracellular or in vivo sensors:

1. The inert matrix protects cellular contents from the incorporated sensing components, and vice versa. The nanoparticle matrix eliminates interferences such as protein binding and membrane/organelle sequestration.
2. Each nanoparticle can be loaded with a high number of sensing components because of its larger size (compared to that of the molecular dyes), enhancing the signal-to-background ratio.
3. Loading of multiple components per nanoparticle can allow ratiometric measurements as well as multiplex sensing or sophisticated synergistic designs. The ratiometric mode of operation assures that measurements are unaffected by excitation intensity, absolute concentration, and sources of optical loss, which is essential for intensity-based intracellular or in vivo measurements wherein there are many interfering factors.
4. Nanoparticles can be surface-coated with biological molecules such as proteins and peptides for targeting to specific cells or for sensor designs (18). They can also be coated with polyethylene glycol (PEG) for reduced nonspecific binding and longer plasma half-life. Such surface modification is especially useful for in vivo sensing, as it helps to increase the accumulation of nanoparticles at the location of interest.
5. Nanoparticles have a high surface-to-volume ratio, resulting in high analyte/target accessibility to the indicator dyes/receptors. In some cases, high loaded amounts of dyes in close proximity to one another—either within the nanoparticle matrix or on its surface—can allow multiple interactions with the sensing components, leading to signal amplification (19). Notably, similar amplification effects have been reported for the targeting efficiency of nanoparticles with multiple surface-conjugated targeting moieties (20).

QD: quantum dot

Photobleaching: the photochemical destruction of a dye, resulting in color and fluorescence bleaching

LSPR: localized surface plasmon resonance

SERS: surface-enhanced Raman scattering

SPIO: superparamagnetic iron oxide

PEBBLE: photonic explorer for biomedical use with biologically localized embedding

PAA: polyacrylamide

6. Some types of nanoparticles possess unique but controllable optical/magnetic properties that are superior to molecular probes. For example, semiconductor nanoparticles, commonly known as quantum dots (QDs), have large fluorescence quantum yields, are resistant to photobleaching, and have good chemical stability. The optical properties of QDs can be tuned by controlling the size, composition, and preparation procedures. Metal nanoparticles or metal nanoshells coated on polymer nanoparticles have localized surface plasmon resonance (LSPR) and induce surface-enhanced Raman scattering (SERS) that is free from photobleaching (21). The LSPR wavelength of the metallic nanoparticles can be tuned by changing the shape, size, and composition of the metal nanoparticle or the thickness of the metal shell (22, 23). Superparamagnetic iron oxides (SPIOs) provide negative contrast enhancement for magnetic resonance imaging (MRI). These characteristics can be utilized for constructing various multiplex sensors.

A wide variety of nanoparticle sensors have been reported since the development of the nano-PEBBLE (photonic explorer for biomedical use with biologically localized embedding) by Kopelman and colleagues (24, 25) more than a decade ago. Some nanoparticle sensors have been developed for intracellular or in vivo measurements of (*a*) metabolites such as ions and small molecules and (*b*) cell-related processes and forces. Some of these sensors have been developed for large molecules such as proteins and nucleic acids and are primarily used in laboratory diagnostic assays in body fluids or tissues. Note that this nanoparticle platform concept has been extended to the design of nanomedical tools (such as nanotheranostic devices), wherein the nanoparticle is loaded with contrast imaging agents and/or therapeutic agents instead of sensing elements (17, 26, 27). In vivo applications of medical nanoparticle devices have been successful in cancer imaging and therapy (14, 17, 28) when aided by an EPR (enhanced permeability and retention) effect (29), which allows preferential accumulation at tumor sites due to nanoparticles' size advantage. The nanodevices showed an enhanced targeting efficiency when they were surface-conjugated with targeting moieties specific to the overly expressed proteins in tumor cells or vasculatures (14, 30, 31).

This review focuses on the design, properties, and applications of nanoparticle-based bioanalytical sensors for small molecules and ions, with an emphasis on in situ measurements in live cells and in vivo. Nanoparticle sensors for large molecules are not discussed, as they have been developed mainly for laboratory diagnosis assays (32–35). Mechanically fixed nanosensors such as fiber-tip devices have made historical contributions to live-cell sensing (36), but they are little used now. Film-on-glass-slide and microarray-on-a-chip sensors, even when they utilize nanoparticles, are rarely suitable for intracellular or in vivo measurements; therefore, we do not discuss them here.

2. NANOPARTICLE SENSORS: DESIGN AND PREPARATION

A typical nanoparticle sensor design uses the nanoparticle as a chemically inert platform loaded with sensing components. The sensing mechanism involves the permeation of analytes into the nanoparticle matrix and their selective interaction with sensing components, which results in signal changes. The important properties of sensors, such as sensitivity, dynamic range, selectivity, reversibility, and stability, depend mostly on the incorporated sensing components. However, the nanoparticle matrix also plays an important role: The properties of the matrix, such as pore size, hydrophobicity, and charge, determine the permeability and solubility of the analytes as well as the loading efficiency of the sensing probes (4). For example, polyacrylamide (PAA) nanoparticles have served as good matrices for ion sensors (37–41) due to their neutral and hydrophilic nature, whereas hydrophobic nanoparticle matrices are better suited for oxygen sensors (10, 42). A wide variety of nanoparticle matrices have been used as sensor platforms, including polymer nanoparticles made of organic, inorganic, or organic-inorganic hybrid materials; polymer-capped liposomes or micelles;

semiconductor nanoparticles; and metallic (metal or metal-shell) nanoparticles. The pores of the nanoparticle matrix are sufficiently large to allow diffusion of the smaller analyte ions or molecules (so that the matrix can bind with the molecular probes located inside the nanoparticle), but the pores are still small enough to exclude the diffusion of larger proteins into the core matrix. This exclusion of macromolecules is quite significant because many "naked-molecule" dyes change their fluorescence properties in the presence of proteins. However, the nanoparticle sensors containing these same dyes are not affected by the presence of proteins (37, 39, 42, 43).

Chemiluminescence: the emission of light (luminescence) by the release of energy from a chemical reaction

The sensing components of a nanoparticle typically include indicator and reference dyes or a combination of reporter dyes and analyte-specific ligands/biological receptors. Loading of the sensing components into the nanoparticles is performed either during synthesis or after the formation of the nanoparticles by encapsulation, covalent linkage, bioaffinity interaction such as that between streptavidin and biotin, or physical adsorption through charge-charge or hydrophobic interaction. The covalent linkage is typically made via simple coupling reactions between the nanoparticle functionalized with amine, carboxyl, or thiol groups and the molecules containing similar functional groups. Biological molecules such as antibodies, DNAs, and peptides have been used as receptors because of their highly selective biological interactions. These biomolecular receptors have also been utilized as targeting moieties, enabling nanoparticles to perform real-time tracking of target biomolecules in cells (15) as well as tumor-targeted delivery of drugs or image contrast agents in rodents (14, 17). If targeting moieties are added to nanoparticle sensors, the sensors can even detect specific analytes in a spatially localized target area (44).

QDs, metallic nanoparticles, and SPIOs have been used to form part of a sensing core as well as part of a platform. The optical and magnetic characteristics of these nanoparticles can change in response to specific analytes when the nanoparticles are labeled with suitable dyes, ligands, or receptors.

Figures 2 and **3** show designs of various types of nanoparticle sensors. Most nanoparticle sensors use fluorescence (**Figures 2*a*,*b*,*d*–*f***; **3*a***) as a detection signal, but some use chemiluminescence (**Figure 2*c***), scattering (**Figure 3*b*,*c***), absorbance (**Figure 3*c***), or magnetic resonance (**Figure 3*c***). The properties and in vitro and in vivo applications of each type of nanoparticle sensor are detailed in the following section.

3. NANOPARTICLE SENSORS: PROPERTIES AND APPLICATIONS

3.1. Polymer Nanoparticle Sensors with Fluorescent Indicator Dyes

In the design of polymer nanoparticle sensors with fluorescent indicator dyes (**Figure 2*a***), the fluorescent indicator and reference dyes are loaded into the polymeric nanoparticle core or its surface-coated layer, and there is no interaction between the dyes. Nanoparticle sensors based on this design are used to sense ions (H^+, Ca^{2+}, Mg^{2+}, Zn^{2+}, Fe^{3+}, and K^+) (11, 37–41, 45, 46), radicals (OH radical) (47), small molecules (O_2, singlet oxygen, and H_2O_2) (10, 42, 48–54), and cellular electric fields (55).

3.1.1. Ion sensors. Most ion nanoparticle sensors under this category are PEBBLE sensors, which are made of hydrophilic PAA nanoparticles with encapsulated fluorescent dyes. However, a few different designs have been reported. For example, a pH nanoparticle sensor was prepared using a PAA nanoparticle with covalent linked dyes (45), and a K^+ nanoparticle sensor was made by loading the sensing dye into the surface-coated layer polyelectrolytes instead of into the nanoparticle itself (46). PEBBLE sensors have made successful intracellular measurements for pH, Mg^{+2}, and Ca^{2+} (11, 24, 37, 38). The Mg^{2+} PEBBLE sensor is a particularly interesting example in terms

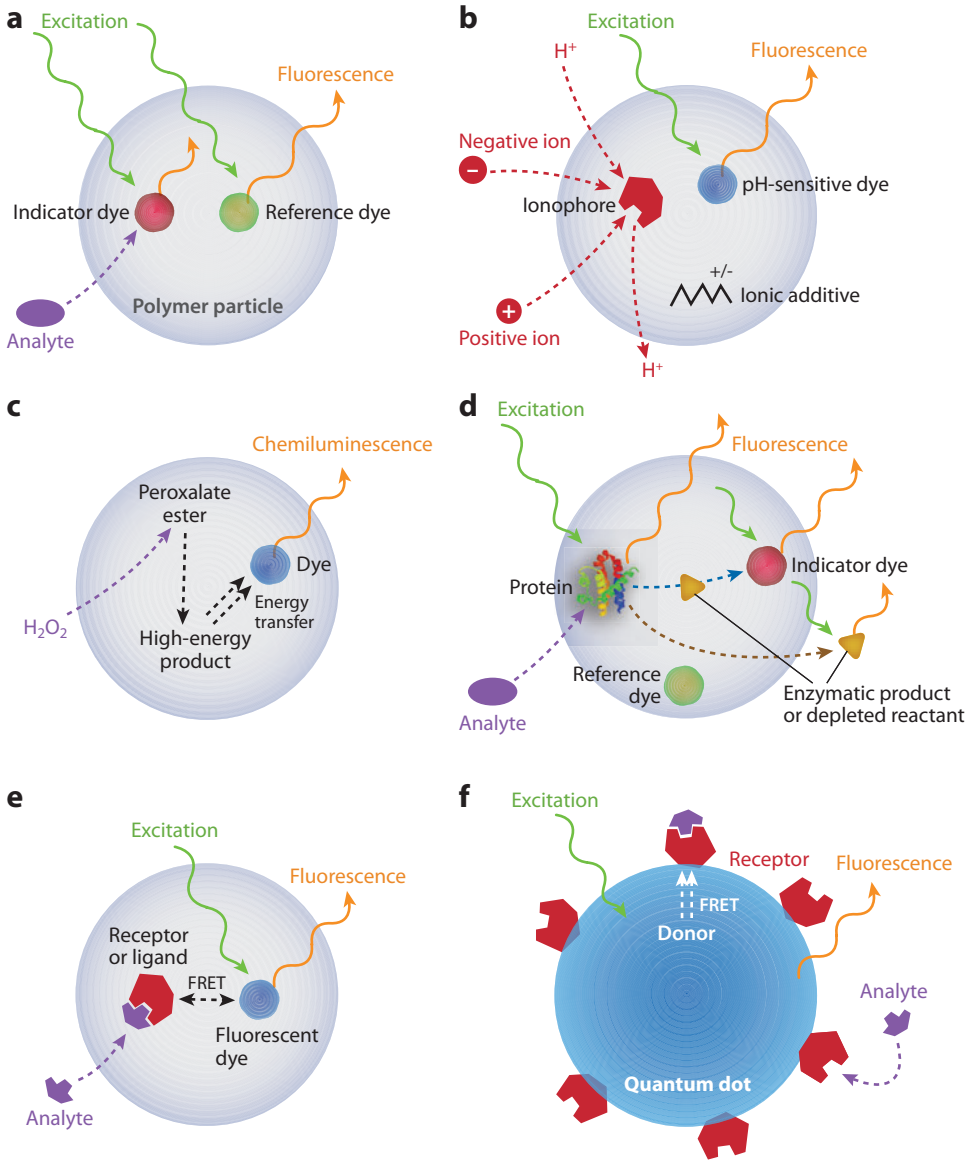

Figure 2

Schematic diagrams of various designs of luminescent nanoparticle sensors. (*a*) Polymer nanoparticle sensor with fluorescent indicator dyes. (*b*) Ion-correlation nanoparticle sensor. (*c*) Chemiluminescence nanoparticle sensor. (*d*) Polymer nanoparticle sensor with encapsulated protein. (*e*) Fluorescence resonance energy transfer (FRET)-based polymer nanoparticle sensor. (*f*) FRET-based quantum dot sensor.

of design and cellular application. It has achieved both high selectivity and high sensitivity through the use of a specific combination of nanoparticle matrix and dyes. The traditional measurement of magnesium ion concentrations in biological environments has suffered from severe interference from calcium ions. Coumarine 343 is a small hydrophilic dye that does not penetrate the cell membrane by itself, but it is a very sensitive Mg^{2+} ion probe: Its selectivity for magnesium over

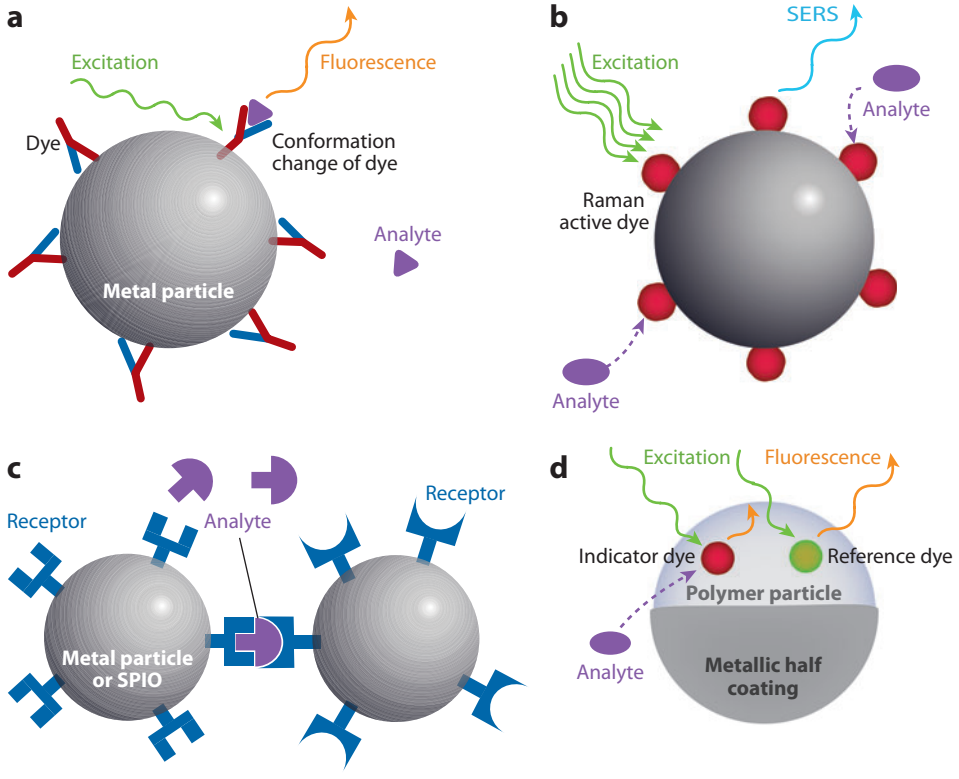

Figure 3

Schematic diagrams of sensor designs using metallic nanoparticles and/or superparamagnetic iron oxides (SPIOs). (*a*) Fluorescent sensor: metallic nanoparticle conjugated with fluorescent receptors. (*b*) Surface-enhanced Raman scattering (SERS) sensor: metallic nanoparticle with surface-coated Raman active indicator dye. (*c*) Localized surface plasmon resonance (LSPR) sensor or magnetic resonance imaging (MRI) sensor: metallic nanoparticles or SPIOs conjugated with receptors. (*d*) Modulated optical nanoprobe sensor. Note that the LSPR or MRI sensor detects the signal change from the aggregation status of the sensors, requiring multiple particles.

calcium is higher than that of any commercially available probe. The Mg^{2+} PEBBLE sensor was constructed by encapsulating this hydrophilic dye and a commercial reference dye (Texas Red) in a hydrophilic PAA nanoparticle (37). The linear response of these PEBBLEs to Mg^{2+} ion, in the range of 0.1 to 10 mM, met with no interference even in the simultaneous presence of 1 mM calcium, 20 mM sodium, and 120 mM potassium. This demonstrated that this Mg^{2+} PEBBLE may reliably indicate intracellular Mg^{2+} concentrations. Indeed, these Mg^{2+} PEBBLEs have been utilized to determine the role of Mg^{2+} inside human macrophage cells in the presence of invading *Salmonella* bacteria (56). The Mg^{2+} measurements made by the PEBBLE sensors showed conclusively that Mg^{2+} is not an important contributor to the control of pathogens by macrophages, in contradiction to previous reports (57).

3.1.2. Dissolved oxygen sensors. The first nanoparticle sensor for dissolved oxygen was the silica-based PEBBLE sensor, which was prepared by embedding $[Ru(dpp)_3]^{2+}$ (a ruthenium oxygen indicator dye) and reference dyes into silica nanoparticles (49). The sensor successfully imaged intracellular oxygen in live C6 glioma cells (**Figure 4**). Oxygen PEBBLE sensors with enhanced

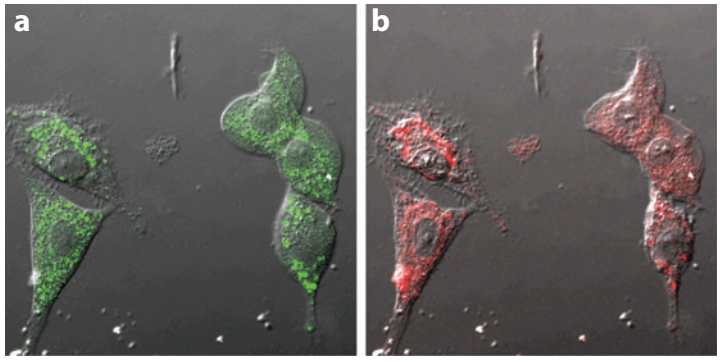

Figure 4

Confocal images of rat C6 glioma cells loaded with sol-gel PEBBLEs (photonic explorers for bioanalysis with biologically localized embedding) by gene gun injection. Nomarski illumination image overlaid with Oregon Green fluorescence (reference, *a*) and $[Ru(dpp)_3]^{2+}$ fluorescence (oxygen indicator, *b*) of the same ratiometric PEBBLEs inside cells. Adapted from Reference 49 with permission from the American Chemical Society.

sensitivity and dynamic range were developed embedding the more sensitive platinum-based oxygen dyes, as well as reference dyes, into a hydrophobic matrix such as organically modified silica (ormosil) (10) or polydecylmethacrylate (PDMA) (42). The hydrophobic matrix is usually better suited for oxygen sensing than is the hydrophilic matrix due to its higher oxygen solubility. These hydrophobic PEBBLE nanosensors exhibit a perfectly linear Stern–Volmer calibration curve over the entire range of dissolved oxygen concentrations, an ideal but previously unachieved goal for any fluorescent oxygen sensor. The sensitivity, represented in the below equation by Q_{DO}, was 97–97.5%, which is the highest reported value. Q_{DO} is the quenching response to dissolved oxygen, defined by

$$Q_{DO} = (I_{N_2} - I_{O_2})/I_{N_2} \times 100,$$

where I_{N_2} is the fluorescence intensity of the indicator dye (or the ratio of indicator dye intensity to reference dye intensity) in fully deoxygenated water, and I_{O_2} is the fluorescence intensity in fully oxygenated water.

The embedded platinum(II) octaethylporphine ketone, another oxygen-sensitive dye, has infrared fluorescence and allows oxygen PEBBLE sensors to operate even in human plasma samples (42) and to remain unaffected by the plasma's notoriously high light scattering and autofluorescence. Oxygen PEBBLE sensors made of ormosil nanoparticles were successfully applied for real-time imaging of oxygen inside live cells, i.e., monitoring metabolic changes inside live C6 glioma cells (10).

Oxygen sensors have also been created by embedding ruthenium dyes into the polyelectrolyte layers on commercial fluorescent nanoparticle surfaces (50) or into polymerized phospholipid vesicles (liposomes) (51). However, the sensitivities of these sensors were only 60% for polyelectrolyte-coated nanoparticle sensors and 76% for polymerized liposome sensors.

The oxygen measurements given above are all based on fluorescence intensity. However, methods such as fluorescence anisotropy (43) and life-time measurement (52, 53) have also been utilized. For example, the oxygen concentration inside green plant cells was measured with nanoparticle sensors injected by glass microcapillaries. The sensors were constructed by encapsulating Pt(II)-tetra-pentafluorophenyl-porphyrin in polystyrene beads measuring 0.3–1 μm in diameter (52). The same sensors were injected into the salivary glands of blowflies to quantify the changes in oxygen content within individual gland tubules during hormone-induced secretory activity (53). The types of sensors discussed in this section are summarized in **Table 1**.

Table 1 Dissolved oxygen nanoparticle sensors

Matrix	Size	Oxygen indicator	Optical signal	Q_{DO}	Reference(s)
Silica	20–300 nm	Ru(II)-tris(4,7-diphenyl -1,10-phenanthroline) dichloride	Fluorescence intensity	80%	49
			Fluorescence anisotropy	N/A	43
Ormosil	120 nm	Pt(II) octaethylporphine ketone	Fluorescence intensity	97%	10
Ormosil	120 nm	Pt(II) octaethylporphine	Fluorescence intensity	97%	10
PDMA	150–250 nm	Pt(II) octaethylporphine ketone	Fluorescence intensity	97.5%	42
Commercial fluorophore coated with polyelectrolyte layers	100 nm	Ru(II)-tris(4,7-diphenyl -1,10-phenanthroline) dichloride	Fluorescence intensity	60%	50
Polymerized liposome	150 nm	Ru(II)-tris(4,7-diphenyl -1,10-phenanthroline) dichloride	Fluorescence intensity	76%	51
Polystyrene	300 nm–1 μm	Pt(II)-tetra-pentafluorophenyl-porphyrin	Fluorescence lifetime	N/A	52, 53

Abbreviations: N/A, not available; ormosil, organically modified silicate; PDMA, polydecylmethacrylate; Q_{DO}, quenching response to dissolved oxygen.

3.1.3. Sensors for reactive oxygen species. Ratiometric PEBBLE sensors were developed for reactive oxygen species (ROS), singlet oxygen, H_2O_2, and hydroxyl radical using irreversible molecular probes. A singlet oxygen PEBBLE sensor was prepared by incorporating the singlet oxygen–sensitive 9,10-dimethyl anthracene or the singlet oxygen–insensitive octaethylporphine into ormosil nanoparticles (48). The nanoparticle matrix enhances the selectivity of the indicator dye to singlet oxygen by blocking the entry of short-lived polar ROS such as OH and superoxide radicals. These nanoprobes have been used to monitor the singlet oxygen produced by dynamic nanoplatforms, which were developed for photodynamic therapy (PDT) (14). Another singlet oxygen PEBBLE sensor was constructed with ormosil nanoparticles incorporating 1,3-diphenylisobenzofuran (DPIBF). The intracellular concentration of singlet oxygen within C6 glioma cells during PDT was measured with the DPIBF sensors (54). A PEBBLE sensor for H_2O_2 was prepared by embedding 2′,7′-dichlorofluorescin diacetate into ormosil nanoparticles. The PEBBLE sensors successfully detected H_2O_2 within a macrophage at a low-nanomolar concentration (54).

A PEBBLE sensor for detecting the OH radical was created by covalently attaching the hydroxyl indicator dye, coumarin-3-carboxylic acid, onto the PAA nanoparticle surface while encapsulating the reference dye deep within the sensor (47). This design circumvents two potential problems posed by the hydroxyl radical, the most reactive ROS: (*a*) its inability to penetrate significantly into any matrix without being destroyed and (*b*) its ability to oxidize (and photobleach) most potential reference dyes. This nanoprobe demonstrated a proof of principle of a ratiometric hydroxyl radical probe and showed good sensitivity and reversibility.

3.1.4. Nanoparticle sensors for electric fields. The E-PEBBLE, a nanosensor designed to measure electric fields, was fabricated by encasing the fast-response, voltage-sensitive fluorescent dye di-4-ANEPPS inside silane-capped (polymerized) micelles (55). The hydrophobic core of the micelle provides a uniform environment for the molecules and thus allows for universal calibration. It also allows for fast orientation of these dye molecules, which shortens the response time. The E-PEBBLEs were introduced into immortalized astrocyte cells (DITNC) by endocytosis, and—for the first time—enabled complete three-dimensional electric-field profiling throughout the entire volume of living cells (not merely inside membranes) (**Figure 5**). Note that traditional

ROS: reactive oxygen species

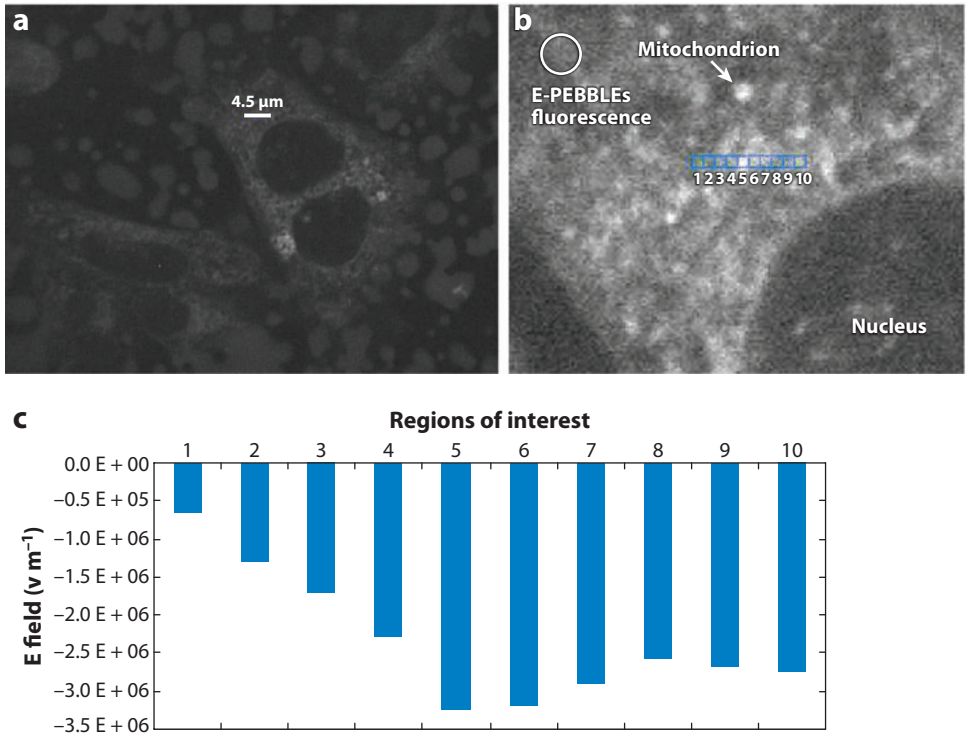

Figure 5

E-PEBBLEs (electric-field photonic explorers for bioanalysis with biologically localized embedding) can measure electric (E) fields in both the cytosolic and the membrane regions of living cells. (*a*) Astrocytes incubated with E-PEBBLEs. The middle cell contains the region analyzed. (*b*) An enlarged image of the cellular regions (membrane and cytosolic) analyzed. An arrow points to a representative mitochondrion. The circular region contains diffuse fluorescence arising from the E-PEBBLEs. The blue pixels (total length: 4.5 μm) indicate the regions analyzed. The regions are numbered 1–10 from left to right. Region 5 contains a mitochondrion (*brightly fluorescent region*), whereas regions 6–10 cross over other mitochondrial regions. The brightness and contrast of this image have been adjusted to 68% and 83% (from 50%, using Microsoft Publisher), respectively, for added clarity. (*c*) A graph showing the E field for the regions analyzed before the addition of CCCP (carbonyl cyanide-m-chlorophenylhydrazone). The highest E field is seen in region 5. Adapted from Reference 55 with permission from the Biophysical Society.

methods such as free-voltage dyes and patch/voltage clamps require calibration steps for each cell or cell type measured and that these measurements are confined to the cellular membranes, which constitute only 0.01% of the cell's volume. The E-PEBBLE's ability to profile the entire cell is expected to greatly enhance our understanding of the role of cellular electric fields in influencing and/or regulating biological processes and will likely have wider implications for cellular biology, biophysics, biochemistry, and medicine.

3.2. Ion-Correlation Nanoparticle Sensors

In this design of ion-sensing nanoparticle sensors (**Figure 2*b***), the hydrophobic polymeric nanoparticle is loaded with three lipophilic components: a highly selective but optically silent ionophore, a pH-sensitive fluorescent dye, and an ionic additive. Ion-correlation nanoparticle sensors have been developed for K^+, Na^+, and Cl^- ions (9, 58–62). Ion sensing is based on the

same mechanism as that for fluorescent ion-selective optodes (63–66). When a selective ionophore binds the ions of interest, thermodynamic equilibrium–based ion exchange (for sensing cations) or ion coextraction (for sensing anions) occurs simultaneously. This exchange/coextraction changes the local pH in proportion to the concentration of the ion of interest within the nanoparticle matrix; the change in pH is then optically detected by the pH-sensitive dye. The ionic additive is used to maintain ionic strength. Note that in a modified design (61), the ions are measured by the bright fluorescence of QDs instead of by pH dye, utilizing the overlap of the emission of the embedded QDs with the absorbance of the pH dye. The hydrophobic nanoparticle matrixes for the ion-correlation sensors include PDMA (9, 58, 59), poly(n-butyl acrylate) (62), and poly(vinyl chloride) (60, 61). The composition of the matrix as well as the ratios of the three sensor components were found to affect sensor characteristics such as dynamic range, selectivity, and response time (9, 62). The ion-correlation nanoparticle sensors are both sensitive and selective. For example, the sensitivity of two K^+ ion–correlation nanoparticle sensors is higher by a factor of 1,000–10,000 than that of the K^+ nanoparticle described in Section 3.1 above (46). PDMA-based PEBBLE sensors have made intracellular measurements for K^+, Na^+, and Cl^- ions. For example, the sensors were delivered by gene gun into rat C6 glioma cells, where they successfully measured an increase in the intracellular K^+ concentration following the addition of kainic acid, a K^+ channel–opening agonist (9).

3.3. Chemiluminescence Nanoparticle Sensors

Chemiluminescence has been utilized to design sensors for H_2O_2 (**Figure 2*c***) (67). Such sensors are made of peroxalate ester nanoparticles and encapsulated fluorescent dyes. The sensing mechanism occurs as follows: H_2O_2 reacts with the peroxalate ester groups, generating a high-energy dioxetanedione that then chemically excites encapsulated fluorescent dyes, leading to chemiluminescence. These sensors have nanomolar sensitivity and excellent specificity (over other ROS) for H_2O_2. The chemiluminescence wavelength can be tuned by changing the encapsulated fluorescent dyes. In one study (67), peroxalate particles containing perylene, rubrene, and pentacene emitted light at wavelengths of 460, 560, and 630 nm, respectively. The nanoparticle sensors with encapsulated pentacene were applied for in vivo imaging of H_2O_2 and were externally injected as well as endogenously produced in the peritoneal cavity of mice during lipopolysaccharide-induced inflammatory response (67).

3.4. Polymer Nanoparticle Sensors with Encapsulated Proteins

Two types of nanosensors operating on different sensing mechanisms have been developed using an encapsulated-protein design (**Figure 2*d***). The first type incorporates an encapsulated protein that behaves as a fluorescent molecular probe. Nanoparticle sensors for copper and phosphate ions are two examples. The $Cu^{+/2+}$ sensor was constructed by incorporating DsRed, red fluorescent protein, and a reference dye into PAA nanoparticles (40). The detection range for Cu^+ and Cu^{2+} was 0.2–5 μM. The phosphate sensor was made of PAA nanoparticles and embedded fluorescent phosphate–sensing proteins and had a micromolar detection range (68). In the second type of sensor, the encapsulated protein is an enzyme that catalyzes the reaction involved with analytes. The enzymatic reaction leads to a change in fluorescence, either by fluorescence product or by coembedded fluorescent indicator dye for depleted reactant. Examples include a glucose sensor and two H_2O_2 sensors. The glucose sensor was developed by incorporating glucose oxidase (GO_x), an oxygen-sensitive ruthenium-based dye, and a reference dye within PAA nanoparticles (69). The enzymatic oxidation of glucose to gluconic acid results in the local depletion of oxygen, which

increases the fluorescence of the encapsulated oxygen-sensitive dye. The dynamic range of these sensors was found to be ~0.3–8 mM, which is suitable for intracellular measurements.

Fluorescence resonance energy transfer (FRET): a distance-dependent energy-transfer mechanism between two dye molecules that occurs via a nonradiative, long-range, dipole-dipole coupling mechanism

The H_2O_2 nanoparticle sensors were developed by encapsulating horseradish peroxidase (HRP) within either PAA (70) or PEG (71) nanoparticles. The PAA-based sensor contains co-embedded fluorescein dye, whose fluorescence intensity decreases when HRP catalyzes the oxidation of dye in the presence of ROS (70). The PEG-based sensor uses externally introduced Amplex Red (10-acetyl-3,7-dihydroxyphenoxazine) for H_2O_2 measurement (71). The encapsulated HRP catalyzes the reaction between Amplex Red and H_2O_2, forming a red fluorescent product termed resorufin in proportion to the amount of H_2O_2. The sensors are phagocytized into macrophages and respond to exogenous H_2O_2 (100 μM) as well as to endogenous H_2O_2 induced by lipopolysaccharide.

3.5. Fluorescence Resonance Energy Transfer–Based Nanoparticle Sensors

Sensors based on the fluorescence resonance energy transfer (FRET) mechanism are typically designed in one of three ways:

1. Polymer nanoparticles are loaded with an analyte-insensitive fluorescent dye and analyte-selective molecules or ligands (**Figure 2*e***).
2. QD sensors are loaded with surface-conjugated analyte-selective molecules or ligands (**Figure 2*f***).
3. Metallic nanoparticles are loaded with surface-conjugated analyte-selective fluorescent molecules or ligands (**Figure 3*a***).

In the third design, the metallic nanoparticle serves as a fluorescence quencher. FRET occurs between the embedded fluorescent dyes/QDs/metal nanoparticle and the analyte-specific molecules/ligands. The fluorescence of the embedded or surface-attached dye or QD is quenched or restored when analytes bind with analyte-specific molecules/receptors. FRET-based nanoparticle sensors have been developed to detect ions and small molecules as well as cellular processes such as apoptosis using polymer and gold nanoparticles, dendrimers, and QDs.

3.5.1. Ions sensors. Copper ions are the ions most frequently studied by FRET-based nanoparticle sensors. Some of these sensors are used solely for Cu^{2+}, but others are used for different ions as well as Cu^{2+}. Reported sensor designs for copper ions include (*a*) silica nanoparticles containing fluorescent dansylamide and a Cu^{2+}-specific picolinamide subunit (72–74), (*b*) latex nanoparticles containing fluorophore BODIPY and copper-chelating receptors (cyclam) (75, 76), (*c*) thioglycerol-capped CdS QDs (77), and (*d*) gold nanoparticles coordinated with fluorescent chromophore-containing pyridyl moieties through weak interactions (78). The sensitivity of the sensors can be tuned by the ratio of ligand to dye (72–74). The response of the sensors is fast: For instance, 90% quenching of fluorescence occurred within 1s for cyclam-conjugated nanoparticle sensors (75, 76).

FRET-based sensors for copper and other ions were created using silica nanoparticles or QDs. The sensors made of silica-containing polyamine chains (the receptors) coupled with dansyl units (the fluorophores) were selective for copper, cobalt, and nickel ions (19). Pentapeptide Gly–His–Leu–Leu–Cys-coated CdS QDs (2.4 ± 1.5 nm, as measured by transmission electron microscopy) were designed for selective detection of Cu^{2+} and Ag^{+} (79). The typical detectable range of Cu^{2+} by these sensors ranges from 0.1 to 1000 uM, and the lowest detection limit—by the latex-based sensor—was 1 nM (75, 76). However, the normal unbound copper ion level inside cells is only in the femtomolar range, which explains why none of the copper ion nanoparticle sensors (both FRET-based sensors and sensors loaded with DsRed protein, described above) has been applied

for intracellular studies. These sensors may be applied for cells under stressed conditions that could increase the free copper ion concentration to micromolar levels (80).

A mercury(II) FRET–based sensor was developed using gold nanoparticles with adsorbed Rhodamine B molecules (81). A high selectivity to Hg(II) against other metal ions was achieved by modifying the sensor with mercaptopropionic acid and adding a chelating ligand, 2,6-pyridinedicarboxylic acid, to the test solutions. The detection limit for Hg(II) was 2.0 ppb.

3.5.2. Sensors for maltose. FRET-based maltose sensors have been developed using QDs, maltose-binding protein (MBP), and a dye complex that forms a FRET pair with QD. In one design (82), the dye complex (composed of β-cyclodextrin–acceptor dye conjugates) is initially bound to MBP, resulting in FRET quenching of the QD fluorescence. Adding maltose displaces the dye complex, increasing the QD fluorescence in proportion to the maltose concentration. The sensors are modified to operate on a two-step FRET mechanism by labeling the MBP with another fluorescent dye so as to overcome inherent QD donor-acceptor distance limitations. In another design (83, 84), a ruthenium dye is covalently linked to MBP and therefore is not displaced by maltose, thus preventing possible errors caused by displaceable dyes. When maltose binds with MBP, however, the interaction (distance) between the Ru complex and the QD changes, leading to a concentration-dependent increase in QD fluorescence.

3.5.3. Apoptosis sensors. A FRET-based nanoparticle sensor for apoptosis was created by conjugating a caspase-specific FRET-based apoptosis reagent (PhiPhiLux G1D2) to a G5 poly(amidoamine) dendrimer. The sensor was conjugated with a targeting moiety (here, folic acid) for detection of specific cell lines (44). The targeted apoptosis measurement by the nanosensors was demonstrated using two different cell lines: KB cells (folate receptor positive) and UMSCC-38 cells (folate receptor negative). When the nanoparticle sensor–treated cells were exposed to the apoptosis-inducing agent staurosporine, they detected apoptosis only in the KB cells, indicating that cell-specific delivery of nanoparticle sensors occurred as a result of surface-conjugated targeting moieties.

3.6. Surface-Enhanced Raman Spectroscopy Sensors or Localized Surface Plasmon Resonance Sensors Using Metallic Nanoparticles

Metallic nanoparticles (also known as metal-core nanoparticles or metal-coated polymer nanoparticles) demonstrate three unique properties: (*a*) fluorescence quenching, (*b*) SERS of surface-bound Raman-active molecules, and (*c*) LSPR. The fluorescence-quenching property has been utilized for FRET-based sensors, as described above (**Figure 3*a***). SERS and LSPR have also been utilized in the design of nanoparticle sensors.

Metallic SERS sensors (**Figure 3*b***) are prepared by labeling metallic nanoparticles with Raman-active dyes that are sensitive to specific analytes such as hydrogen ions (85, 86) and large biological molecules (87). SERS pH sensors are fabricated using silver nanoparticles and gold-nanoshell/silica-core nanoparticles. Sensors made of silver nanoparticles (50–80 nm in diameter) functionalized with para-mercaptobenzoic acid (para-MBA) exhibited a characteristic SERS spectrum corresponding to the pH of the surrounding solution (85). The sensor was sensitive to pH changes within the 6–8 range. To measure intracellular pH, the nanoparticle sensors were delivered into living Chinese hamster ovary cells via passive uptake. The resulting SERS spectrum showed that the pH surrounding the nanoparticle was below 6, which is consistent with the particles being located inside a lysosome (of pH 5). A similar SERS pH sensor was made from a

gold-nanoshell/silica-core nanoparticle coated with a layer of para-MBA (86). This nanosensor was capable of continuously measuring pH in its local vicinity over the pH range of 5.80 to 7.60.

MOON: modulated optical nanoprobe

Metallic LSPR sensors are prepared by conjugating metallic nanoparticles with ligands/receptors. The extinction and scattering spectra of plasmonic nanoparticles show spectral shifts that are sensitive to small changes in the local refractive index. Most organic molecules have a higher refractive index than does buffer solution; thus, when these molecules bind to nanoparticles, the local refractive index increases, causing redshifting of the extinction and scattering spectra (35). Based on this working principle, the LSPR sensor can produce distinctive changes in LSPR upon binding specific biological molecules to receptors on the nanoparticle surface. To date, LSPR sensor designs include thin films on a chip or glass slide; i.e., they contain large collections of nanoparticle sensors for biomarker proteins, rather than a single nanoparticle sensor (35).

3.7. Superparamagnetic Iron Oxide–Based Magnetic Resonance Imaging Sensor

SPIO is a nanoparticle negative contrast agent for MRI. SPIO sensors are prepared by conjugating the nanoparticles with ligands/receptors—the same process used to create metallic LSPR sensors (**Figure 3*c***). The working principle is based on a decrease in SPIOs' local T2 relaxation rates, which is caused by the aggregation of SPIO particles. SPIOs conjugated with receptors/ligands have been developed for the detection of proteins and nucleic acids (88) as well as calcium ions (89). These sensors utilize specific molecular interactions such as DNA-DNA, protein-protein, protein–small molecule, and enzyme reactions. For example, SPIO-based MRI sensors for Ca^{2+} have been developed based on calcium-dependent interactions between the calcium-binding protein calmodulin and a target peptide, M13 or RS20A (89). Two types of bioconjugated SPIOs, SPIOs conjugated with calmodulin and SPIOs conjugated with M13 or RS20A, have been used for MRI monitoring of Ca ions. The calcium response of these sensors is based on selective aggregation of SPIOs in the presence of calcium. Although fully reversible, this response is slow because the aggregation process requires considerable time (several minutes) to reach equilibrium. Note that the response time of the fluorescent Ca sensor is less than 1 ms (38). Despite such disadvantages, the MRI sensor may be useful for measurements in live, opaque specimens because (*a*) its sensing mechanism does not depend on the separation of bound and unbound reagents and (*b*) there is no problem with tissue-penetration depth.

3.8. Modulated Optical Nanoprobe Sensors

MOONs (modulated optical nanoprobes) are metallically half-capped fluorescent nanoparticles. MOONs can be either magnetic (90, 91) (MagMOONs) or nonmagnetic, as are MOONs used for measuring Brownian rotation (92). The magnetically induced periodic motion of the MagMOON (or random thermal motion in the case of Brownian MOONs) modulates the fluorescence signal, enabling the separation of signal from background (**Figure 6**). This simple procedure increases the signal-to-background ratio by several orders of magnitude (90). This technique expands the breadth of applications of fluorescent nanoparticle sensors to include samples with highly scattering and/or fluorescent backgrounds and experiments that use several fluorescent probes. The MOON design can be applied to any fluorescent nanoparticle sensor by adding a metal coating to one hemisphere of the nanoparticle, using either a magnetic particle or a magnetic-coating metal for making MagMOONS. Moreover, the rotation behavior of a MOON can be utilized for local viscosity measurements (93, 94). A MOON sensor constructed with incorporated fluorescent pH indicator dye molecules can perform simultaneous measurements of chemical properties and physical properties (94). Furthermore, the orientation and position of a MOON sensor can

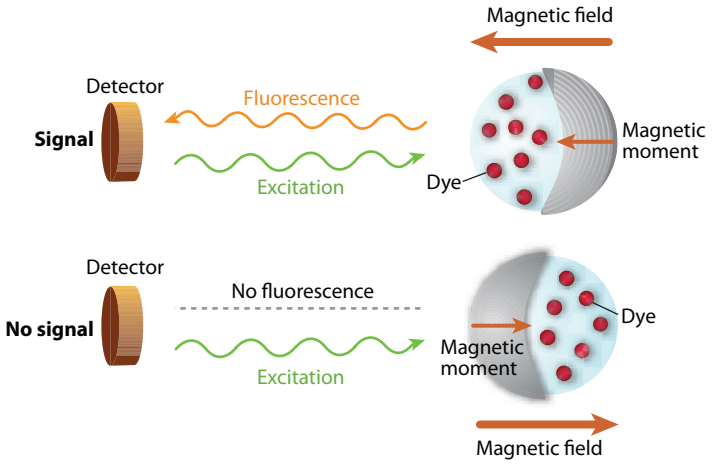

Figure 6

Background-free measurement taken by a magnetically modulated optical nanoprobe (MagMOON). An external magnetic field orients the MagMOON, causing its fluorescent excitation and observed emission to blink on and off as it rotates. Note that the background fluorescence does not blink.

be remotely controlled by an external magnetic field, enabling spatially localized measurements (95). However, MOON sensors have not yet been applied quantitatively for intracellular or in vivo measurements because to date they have been developed using micrometer-sized particles due to the difficulties of efficiently magnetizing and coating of smaller sensor particles. Following recent progress in nanotechnology and coating technology, such as molecular beam epitaxy, nanometer-sized MOONs are being developed (96).

SUMMARY POINTS

1. The nanoparticle platform has the following advantages for intracellular and in vivo sensing: (*a*) physical noninvasiveness due to its small size; (*b*) chemical noninvasiveness due to its inert, nontoxic matrix; (*c*) high accessibility of analytes because of high surface-to-volume ratio; (*d*) ability to control the loading of sensing or targeting moieties per nanoparticle and to modify the surface properties; (*e*) potential for multiplexing and synergistic sensor designs that are not possible with molecular probes; (*f*) potential for targeted delivery to specific cells and/or specific cell compartments; (*g*) prevention of sequestration into certain cell compartments; (*h*) in vivo, prevention of uptake by the immune system; (*i*) in vivo, preferential tumor accumulation due to EPR effect; (*j*) in vivo, ability to cross barriers, such as the blood-brain barrier; and (*k*) inability to be pumped back out of cancer cells, thereby avoiding the multidrug resistance effect.
2. Nanoparticle sensors can detect ions (H^+, Ca^{2+}, Mg^{2+}, K^+, Na^+, Cl^-, phosphate ions, Fe^{3+}, Zn^{2+}, Cu^+/Cu^{2+}, Ag^+, and Hg^{2+}), small molecules (O_2, singlet oxygen, glucose, H_2O_2, and maltose), hydroxyl radicals, electrical fields, viscosity, and apoptosis. Types of nanoparticle sensors include polymer nanoparticles with incorporated fluorescent dyes, ion-correlation nanoparticle sensors, polymer nanoparticles with embedded proteins, chemiluminescence sensors, FRET-based sensors, metallic nanoparticle SERS sensors, metallic nanoparticle LSPR sensors, SPIO MRI sensors, and MOON sensors.

3. Some of the nanoparticle sensors described herein have been successfully applied for intracellular or in vivo measurement, but others have not because of insufficient sensitivity and/or selectivity. Intracellular measurements have been achieved for the following analytes: ions (H^+, Ca^{2+}, Mg^{2+}, K^+, Na^+, and Cl^-), small molecules (O_2, singlet oxygen, and H_2O_2), electrical fields, and apoptosis. In vivo measurements have been reported only for H_2O_2.

FUTURE ISSUES

1. Single-cell analysis can diagnose disease at an early stage, when tissue-level changes are not yet evident but chemical changes within cells are observable (97). Obtaining chemical or physical information from a single cell or a specific location within a single cell is an important future application of nanoparticle sensors.
2. The detection of multiple signals using single-nanoparticle platforms is another future application, as it would enable a diversity of simultaneous experiments and better controls.
3. The in vitro and in vivo applications of nanoparticle sensors have been limited to a few analytes, despite the existence of nanoparticle sensors designed for more diverse analytes. In order to achieve a wider application of nanoparticle sensors (in addition to those applications suggested above), we must improve the sensors' performance, specifically their signal intensity, sensitivity, and selectivity.
4. Promising future directions and opportunities for nanoparticle sensor improvements may include (*a*) improvement of sensing components, specifically developing more sensitive NIR-sensing dyes, receptors that are more selective to analytes/targets, and nanoparticle matrix/surface coatings for longer plasma circulation time; (*b*) adoption of MOON-type sensor designs for signal-to-background ratio enhancement; (*c*) use of remote steering via magnetic or laser tweezers for spatial localization; and (*d*) more enzyme-based sensor stratagems to improve both sensitivity and selectivity.

DISCLOSURE STATEMENT

The authors are not aware of any affiliations, memberships, funding, or financial holdings that might be perceived as affecting the objectivity of this review.

ACKNOWLEDGMENTS

This work was supported by NIH Grants 1R01-EB-007977–01, R21/R33 CA125297 and 1R41 CA 130518-01A1 as well as NSF Grant DMR 0455330.

LITERATURE CITED

1. Cullum BM, Vo-Dinh T. 2000. The development of optical nanosensors for biological measurements. *Trends Biotechnol.* 18:388–93
2. Haugland RP. 2005. *The Handbook: A Guide to Fluorescent Probes and Labeling Technologies*. Eugene, OR: Molecular Probes, Inc. 10th ed.

3. Buck SM, Koo YEL, Park E, Xu H, Philbert MA, et al. 2004. Optochemical nanosensor PEBBLEs: photonic explorers for bioanalysis with biologically localized embedding. *Curr. Opin. Chem. Biol.* 8:540–46
4. Koo YEL, Agayan R, Philbert MA, Rehemtulla A, Ross BD, Kopelman R. 2007. Photonic explorers based on targeted multifunctional nanoplatforms: in vitro and in vivo biomedical applications. In *New Approaches in Biomedical Spectroscopy*, ed. K Kneipp, R Aroca, H Kneipp, E. Wentrup-Byrne, 14:200–18. New York: Am. Chem. Soc.
5. Cheong WF, Prahl SA, Welch AJ. 1990. A review of the optical properties of biological tissues. *IEEE J. Quantum Electron.* 26:2166–85
6. Delpy DT, Cope M. 1997. Quantification in tissue near-infrared spectroscopy. *Phil. Trans. R. Soc. Lond. B* 352:649–59
7. Ntziachristos V, Bremer C, Weissleder R. 2003. Fluorescence imaging with near-infrared light: new technological advances that enable in vivo molecular imaging. *Eur. Radiol.* 13:195–208
8. Woods LA, Powell PR, Paxon TL, Ewing AG. 2005. Analysis of mammalian cell cytoplasm with electrophoresis in nanometer inner diameter capillaries. *Electroanalysis* 17:1192–97
9. Brasuel M, Kopelman R, Miller TJ, Tjalkens R, Philbert MA. 2001. Fluorescent nanosensors for intracellular chemical analysis: decyl methacrylate liquid polymer matrix and ion-exchange-based potassium PEBBLE sensors with real-time application to viable rat C6 glioma cells. *Anal. Chem.* 73:2221–28
10. Koo YEL, Cao Y, Kopelman R, Koo SM, Brasuel M, Philbert MA. 2004. Real-time measurements of dissolved oxygen inside live cells by ormosil (organically modified silicate) fluorescent PEBBLE nanosensors. *Anal. Chem.* 76:2498–505
11. Clark HA, Hoyer M, Parus S, Philbert MA, Kopelman R. 1999. Optochemical nanosensors and subcellular applications in living cells. *Mikrochim. Acta* 131:121–28
12. Chan WCW, Nie SM. 1998. Quantum dot bioconjugates for ultrasensitive nonisotopic detection. *Science* 281:2016–18
13. Akerman ME, Chan WCW, Laakkonen P, Bhatia SN, Ruoslahti R. 2002. Nanocrystal targeting in vivo. *Proc. Natl. Acad. Sci. USA* 99:12617–21
14. Reddy GR, Bhojani MS, McConville P, Moody J, Moffat BA, et al. 2006. Vascular targeted nanoparticles for imaging and treatment of brain tumors. *Clin. Cancer Res.* 12:6677–86
15. Kumar S, Harrison N, Richards-Kortum R, Sokolov K. 2007. Plasmonic nanosensors for imaging intracellular biomarkers in live cells. *Nano Lett.* 7:1338–43
16. Tang W. 2007. *Development and in vitro investigation of methylene blue–containing nanoparticle platforms for photodynamic therapy*. PhD thesis. Univ. Mich., Ann Arbor. 130 pp.
17. Koo YEL, Reddy GR, Bhojani M, Schneider R, Philbert MA, et al. 2006. Brain cancer diagnosis and therapy with nano-platforms. *Adv. Drug Deliv. Rev.* 58:1556–77
18. Clark HAG, Merritt G, Kopelman R. 2000. Novel optical biosensors using a gold colloid monolayer substrate. *Proc. SPIE (Int. Soc. Opt. Eng.)* 3922:138–46
19. Montalti M, Prodi L, Zaccheroni N. 2005. Fluorescence quenching amplification in silica nanosensors for metal ions. *J. Mater. Chem.* 15:2810–14
20. Montet X, Funovics M, Montet-Abou K, Weissleder R, Josephson L. 2006. Multivalent effects of RGD peptides obtained by nanoparticle display. *J. Med. Chem.* 49:6087–93
21. Kneipp K, Kneipp H, Itzkan I, Dasari RR, Feld MS. 2002. Surface-enhanced Raman scattering and biophysics. *J. Phys. Condens. Matter* 14:R597–624
22. Gobin AM, Lee MH, Halas NJ, James WD, Drezek RA, West JL. 2007. Near-infrared resonant nanoshells for combined optical imaging and photothermal cancer therapy. *Nano Lett.* 7:1929–34
23. Jensen TR, Malinsky MD, Haynes CL, Van Duyne RP. 2000. Nanosphere lithography: tunable localized surface plasmon resonance spectra of silver nanoparticles. *J. Phys. Chem. B* 104:10549–56
24. Clark HA, Barker SLR, Brasuel M, Miller MT, Monson E, et al. 1998. Subcellular optochemical nanobiosensors: probes encapsulated by biologically localised embedding (PEBBLEs). *Sens. Actuators B* 51:12–16
25. Sasaki K, Shi ZY, Kopelman R, Masuhara H. 1996. Three-dimensional pH microprobing with an optically-manipulated fluorescent particle. *Chem. Lett.* 25:141–42

26. Harrell JA, Kopelman R. 2000. Biocompatible probes measure intracellular activity. *Biophotonics Int.* 7:22–24
27. Koo YEL, Fan W, Hah HJ, Kopelman R, Xu H, et al. 2007. Photonic explorers based on multifunctional nano-platforms for biosensing and photodynamic therapy. *Appl. Opt.* 46:1924–30
28. Rhyner MN, Smith AM, Gao XH, Mao H, Yang LL, Nie SM. 2006. Quantum dots and multifunctional nanoparticles: new contrast agents for tumor imaging. *Nanomedicine* 1:209–17
29. Maeda H. 2001. The enhanced permeability and retention (EPR) effect in tumor vasculature: the key role of tumor-selective macromolecular drug targeting. *Adv. Enzym. Regul.* 41:189–207
30. Gao X, Cui Y, Levenson RM, Chung LWK, Nie S. 2004. In vivo cancer targeting and imaging with semiconductor quantum dots. *Nat. Biotechnol.* 22:969–76
31. Cai W, Shin D, Chen K, Gheysens O, Cao Q, et al. 2006. In vivo targeting and imaging of tumor vasculature using arginine-glycine-aspartic acid (RGD) peptide-labeled quantum dots. *Nano Lett.* 6:669–76
32. Penn SG, Hey L, Natan MJ. 2003. Nanoparticles for bioanalysis. *Curr. Opin. Chem. Biol.* 7:609–15
33. Kubik TK, Bogunia-Kubik K, Sugisaka M. 2005. Nanotechnology on duty in medical applications. *Curr. Pharm. Biotechnol.* 6:17–33
34. Fischer NO, Tarasow TM, Tok JBH. 2007. Heightened sense for sensing: recent advances in pathogen immunoassay sensing platforms. *Analyst* 132:187–91
35. Anker JN, Hall WP, Lyandres O, Shah NC, Zhao J, Van Duyne RP. 2008. Biosensing with plasmonic nanosensors. *Nat. Mater.* 7:442–53
36. Kopelman R, Tan W. 1993. Near-field optics: imaging single molecules. *Science* 262:1382–84
37. Park EJ, Brasuel M, Behrend C, Philbert MA, Kopelman R. 2003. Ratiometric optical PEBBLE nanosensors for real-time magnesium ion concentrations inside viable cells. *Anal. Chem.* 75:3784–91
38. Clark HA, Hoyer M, Philbert MA, Kopelman R. 1999. Optical nanosensors for chemical analysis inside single living cells. 1. Fabrication, characterization, and methods for intracellular delivery of PEBBLE sensors. *Anal. Chem.* 71:4831–36
39. Sumner JP, Aylott JW, Monson E, Kopelman R. 2002. A fluorescent PEBBLE nanosensor for intracellular free zinc. *Analyst* 127:11–16
40. Sumner JP, Westerberg N, Stoddard AK, Fierke CA, Kopelman R. 2005. Cu^{+} and Cu^{2+} sensitive PEBBLE fluorescent nanosensors using DsRed as the recognition element. *Sens. Actuators B* 113:760–67
41. Sumner JP, Kopelman R. 2005. Alexa Fluor 488 as an iron sensing molecule and its application in PEBBLE nanosensors. *Analyst* 130:528–33
42. Cao Y, Koo YL, Kopelman R. 2004. Poly(decyl methacrylate)-based fluorescent PEBBLE swarm nanosensors for measuring dissolved oxygen in biosamples. *Analyst* 129:745–50
43. Horvath T, Monson E, Sumner J, Xu H, Kopelman R. 2002. Use of steady-state fluorescence anisotropy with PEBBLE nanosensors for chemical analysis. *Proc. SPIE (Int. Soc. Photonic Eng.)* 4626:482–92
44. Myc A, Majoros IJ, Thomas TP, Baker JR. 2007. Dendrimer-based targeted delivery of an apoptotic sensor in cancer cells. *Biomacromolecules* 8:13–18
45. Almdal K, Sun HH, Poulsen AK, Arleth L, Jakobsen I, et al. 2006. Fluorescent gel particles in the nanometer range for detection of metabolites in living cells. *Polym. Adv. Technol.* 17:790–93
46. Brown JQ, McShane MJ. 2005. Core-referenced ratiometric fluorescent potassium ion sensors using self-assembled ultrathin films on europium nanoparticles. *IEEE Sens. J.* 5:1197–205
47. King M, Kopelman R. 2003. Development of a hydroxyl radical ratiometric nanoprobe. *Sens. Actuators B* 90:76–81
48. Cao Y, Koo YEL, Koo S, Kopelman R. 2005. Ratiometric singlet oxygen nano-optodes and their use for monitoring photodynamic therapy nanoplatforms. *Photochem. Photobiol.* 81:1489–98
49. Xu H, Aylott JW, Kopelman R, Miller TJ, Philbert MA. 2001. A real-time ratiometric method for the determination of molecular oxygen inside living cells using sol-gel-based spherical optical nanosensors with applications to rat C6 glioma. *Anal. Chem.* 73:4124–33
50. Guice KB, Caldorera ME, McShane MJ. 2005. Nanoscale internally referenced oxygen sensors produced from self-assembled nanofilms on fluorescent nanoparticles. *J. Biomed. Opt.* 10:064031
51. Cheng ZL, Aspinwall CA. 2006. Nanometre-sized molecular oxygen sensors prepared from polymer stabilized phospholipid vesicles. *Analyst* 131:236–43

52. Schmälzlin E, van Dongen JT, Klimant I, Marmodée B, Steup M, et al. 2005. An optical multifrequency phase-modulation method using microbeads for measuring intracellular oxygen concentrations in plants. *Biophys. J.* 89:1339–45
53. Schmälzlin E, Walz B, Klimant I, Schewe B, Löhmannsröben HG. 2006. Monitoring hormone-induced oxygen consumption in the salivary glands of the blowfly, *Calliphora vicina*, by use of luminescent microbeads. *Sens. Actuators B* 119:251–54
54. Kim G. 2008. *Development of nanoparticle based tools for reactive oxygen species and related biomedical applications*. PhD thesis. Univ. Mich., Ann Arbor. 151 pp.
55. Tyner KM, Kopelman R, Philbert MA. 2007. "Nanosized voltmeter" enables cellular-wide electric field mapping. *Biophys. J.* 93:1163–74
56. Martin-Orozco N, Touret N, Zaharik ML, Park E, Kopelman R, et al. 2006. Visualization of vacuolar acidification–induced transcription of genes of pathogens inside macrophages. *Mol. Biol. Cell* 17:498–510
57. Vescovi EG, Soncini FC, Groisman EA. 1996. Mg^{2+} as an extracellular signal: environmental regulation of *Salmonella* virulence. *Cell* 84:165–74
58. Brasuel M, Kopelman R, Kasman I, Miller TJ, Philbert MA. 2002. Ion concentrations in live cells from highly selective ion correlation fluorescent nano-sensors for sodium. *Proc. IEEE Sens.* 1:288–92
59. Brasuel MG, Miller TJ, Kopelman R, Philbert MA. 2003. Liquid polymer nano-PEBBLEs for Cl analysis and biological applications. *Analyst* 128:1262–67
60. Dubach JM, Harjes DI, Clark HA. 2007. Fluorescent ion-selective nanosensors for intracellular analysis with improved lifetime and size. *Nano Lett.* 7:1827–31
61. Dubach JM, Harjes DI, Clark HA. 2007. Ion-selective nano-optodes incorporating quantum dots. *J. Am. Chem. Soc.* 129:8418–19
62. Ruedas-Rama MJ, Hall EAH. 2007. K^+-selective nanospheres: maximizing response range and minimizing response time. *Analyst* 131:1282–91
63. Bühlmann P, Pretsch E, Bakker E. 1998. Carrier-based ion-selective electrodes and bulk optodes. 2. Ionophores for potentiometric and optical sensors. *Chem. Rev.* 98:1593–687
64. Shortreed MR, Bakker E, Kopelman R. 1996. Miniature sodium selective ion-exchange optode with fluorescent pH chromoionophores and tunable dynamic range. *Anal. Chem.* 68:2656–62
65. Shortreed MR, Barker SLR, Kopelman R. 1996. Anion-selective liquid-polymer optodes with fluorescent pH chromoionophores, tunable dynamic range and diffusion enhanced lifetimes. *Sens. Actuators B* 35:217–21
66. Shortreed MR, Dourado S, Kopelman R. 1997. Development of a fluorescent optical potassium-selective ion sensor with ratiometric response for intracellular applications. *Sens. Actuators B* 38:8–12
67. Lee D, Khaja S, Velasquez-Castano JC, Dasari M, Sun C, et al. 2007. In vivo imaging of hydrogen peroxide with chemiluminescent nanoparticles. *Nat. Mater.* 6:765–69
68. Sun HH, Scharff-Poulsen AM, Gu H, Jakobsen I, Kossmann JM, et al. 2008. Phosphate sensing by fluorescent reporter proteins embedded in polyacrylamide nanoparticles. *ACS Nano* 2:19–24
69. Xu H, Aylott JW, Kopelman R. 2002. Fluorescent nano-PEBBLE sensors designed for intracellular glucose imaging. *Analyst* 127:1471–77
70. Poulsen AK, Scharff-Poulsen AM, Olsen LF. 2007. Horseradish peroxidase embedded in polyacrylamide nanoparticles enables optical detection of reactive oxygen species. *Anal. Biochem.* 366:29–36
71. Kim SH, Kim B, Yadavalli VK, Pishko MV. 2005. Encapsulation of enzyme within polymer spheres to create optical nanosensors for oxidative stress. *Anal. Chem.* 77:6828–33
72. Brasola E, Mancin F, Rampazzo E, Tecilla P, Tonellato U. 2003. A fluorescence nanosensor for Cu^{2+} on silica particles. *Chem. Commun.* 24:3026–27
73. Rampazzo E, Brasola E, Marcuz S, Mancin F, Tecilla P, Tonellato U. 2005. Surface modification of silica nanoparticles: a new strategy for the realization of self-organized fluorescent chemosensors. *J. Mater. Chem.* 15:2687–96
74. Arduini M, Marcuz S, Montolli M, Rampazzo E, Mancin F, et al. 2005. Turning fluorescent dyes into Cu(II) nanosensors. *Langmuir* 21:9314–21
75. Méallet-Renault R, Pansu R, Amigoni-Gerbier S, Larpent C. 2004. Metal-chelating nanoparticles as selective fluorescent sensor for Cu^{2+}. *Chem. Commun.* 20:2344–45

76. Méallet-Renault R, Hérault A, Vachon JJ, Pansu RB, Amigoni-Gerbier S, Larpent C. 2006. Fluorescent nanoparticles as selective Cu(II) sensors. *Photochem. Photobiol. Sci.* 5(3):300–10
77. Chen YF, Rosenzweig Z. 2002. Luminescent CdS quantum dots as selective ion probes. *Anal. Chem.* 74:5132–38
78. He X, Liu H, Li Y, Wang S, Li Y, et al. 2005. Nanoparticle-based fluorometric and colorimetric sensing of copper(II) ions. *Adv. Mat.* 17:2811–15
79. Gattas-Asfura KM, Leblane RM. 2003. Peptide-coated CdS quantum dots for the optical detection of copper(II) and silver(I). *Chem. Commun.* 21:2684–85
80. Bush AI. 2000. Metals and neuroscience. *Curr. Opin. Chem. Biol.* 4:184–91
81. Huang CC, Chang HT. 2006. Selective gold-nanoparticle-based "turn-on" fluorescent sensors for detection of mercury(II) in aqueous solution. *Anal. Chem.* 78:8332–38
82. Medintz IL, Clapp AR, Mattoussi H, Goldman ER, Fisher B, Mauro JM. 2003. Self-assembled nanoscale biosensors based on quantum dot FRET donors. *Nat. Mater.* 2:630–38
83. Sandros MG, Gao D, Benson DE. 2005. A modular nanoparticle–based system for reagentless small molecule biosensing. *J. Am. Chem. Soc.* 127:12198–99
84. Sandros MG, Shete V, Benson DE. 2006. Selective, reversible, regentless maltose biosensing with core-shell semiconducting nanoparticles. *Analyst* 131:229–35
85. Talley CE, Jusinski L, Hollars CW, Lane SM, Huser T. 2004. Intracellular pH sensors based on surface-enhanced Raman scattering. *Anal. Chem.* 76:7064–68
86. Bishnoi SW, Rozell CJ, Levin CS, Gheith MK, Johnson BR, et al. 2006. All-optical nanoscale pH meter. *Nano Lett.* 6:1687–92
87. Cao YC, Jin R, Mirkin CA. 2002. Nanoparticles with Raman spectroscopic fingerprints for DNA and RNA detection. *Science* 297:1536–40
88. Perez JM, Josephson L, O'Loughlin T, Hogemann D, Weissleder R. 2002. Magnetic relaxation switches capable of sensing molecular interactions. *Nat. Biotechnol.* 20:816–20
89. Atanasijevic T, Shusteff M, Fam P, Jasanoff A. 2006. Calcium-sensitive MRI contrast agents based on superparamagnetic iron oxide nanoparticles and calmodulin. *Proc. Natl. Acad. Sci. USA* 103:14707–12
90. Anker JN, Kopelman R. 2003. Magnetically modulated optical nanoprobes. *Appl. Phys. Lett.* 82:1102–4
91. Anker JN, Behrend C, Kopelman R. 2003. Aspherical magnetically modulated optical nanoprobes (MagMOONs). *J. Appl. Phys.* 93:6698–700
92. Behrend CJ, Anker JN, Kopelman R. 2004. Brownian modulated optical nanoprobes. *Appl. Phys. Lett.* 84:154–56
93. Behrend CJ, Anker JN, McNaughton BH, Kopelman R. 2005. Microrheology with modulated optical nanoprobes (MOONs). *J. Magn. Magn. Mater.* 293:663–70
94. McNaughton BH, Agayan RR, Wang JX, Kopelman R. 2007. Physiochemical microparticle sensors based on nonlinear magnetic oscillations. *Sens. Actuators B* 121:330–40
95. Anker JN, Koo YE, Kopelman R. 2007. Magnetically controlled sensor swarms. *Sens. Actuators B* 121: 83–92
96. McNaughton BH. 2007. *Magnetic micro and nano nonlinear oscillators with applications to the dynamic detection of a single bacterium and to physical and chemical sensing*. PhD thesis. Univ. Mich., Ann Arbor. 113 pp.
97. Soper SA, Brown K, Ellington A, Frazier B, Garcia-Manero G, et al. 2006. Point-of-care biosensor systems for cancer diagnostics/prognostics. *Biosens. Bioelectron.* 21:1932–42

Annual Review of
Analytical Chemistry

Volume 2, 2009

Contents

Errata

An online log of corrections to *Annual Review of Analytical Chemistry* articles may be found at http://anchem.annualreviews.org/errata.shtml